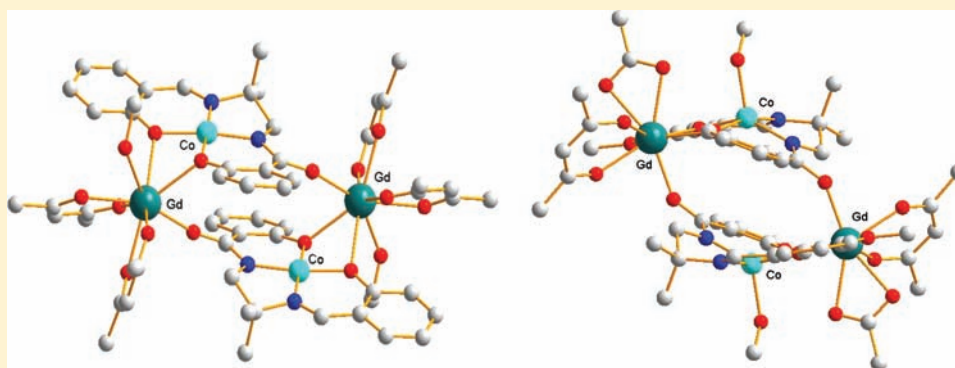


Tetranuclear [Co–Gd]₂ Complexes: Aiming at a Better Understanding of the 3d–Gd Magnetic InteractionVerónica Gómez,^{†,‡,§} Laure Vendier,^{†,‡} Montserrat Corbella,[§] and Jean- Pierre Costes^{*,†,‡}[†]Laboratoire de Chimie de Coordination du CNRS, 205, route de Narbonne, BP 44099, F-31077 Toulouse Cedex 4, France[‡]Université de Toulouse, UPS, INPT, F-31077 Toulouse Cedex 4, France[§]Departament de Química Inorgànica, Universitat de Barcelona, Martí i Franquès 1-11, 08028-Barcelona, Spain

S Supporting Information



ABSTRACT: Tetranuclear [Co–Gd]₂ complexes were prepared by using trianionic ligands possessing amide, imine, and phenol functions. The structural determinations show that the starting cobalt complexes present square planar or square pyramidal environments that are preserved in the final tetranuclear [Co–Gd]₂ complexes. These geometrical modifications of the cobalt coordination spheres induce changes in the cobalt spin ground states, going from $S = 1/2$ in the square planar to $S = 3/2$ for the square pyramidal environments. Depending on the ligand, the complexes display antiferromagnetic or ferromagnetic Co^{II}–Gd^{III} interactions. The temperature dependence of the magnetic susceptibility–temperature products indicate that the Co–Gd interaction is ferromagnetic when high spin Co ions are concerned and antiferromagnetic in the case of low spin Co ions. This different magnetic behavior can be explained if we observe that the singly occupied σ $d_{x^2-y^2}$ orbital is populated ($S = 3/2$ Co ions) or unoccupied ($S = 1/2$ Co ions). Such an observation furnishes invaluable information for the understanding of the more general 3d–4f magnetic interactions.

■ INTRODUCTION

The syntheses of 3d–4f complexes became more popular during these past years because of the wide interest in single-molecule magnets (SMMs),¹ species characterized by their high spin states and their negative axial anisotropy. Indeed it is easy to bring anisotropy into complexes or clusters by introduction of 4f ions while high spin species can be obtained by increasing the number of metal ions in the cluster. Unfortunately, the study of the magnetic interactions between the 3d and 4f ions constituting the cluster is not facilitated as several interaction pathways between the 3d–3d, 3d–4f, and 4f–4f ions are present and active. On the contrary, the preparation of complexes containing only a limited number of 3d and 4f ions is crucial when the study is oriented toward a better understanding of the 3d–4f magnetic interactions. In such a case, the best example is a simple heterodinuclear 3d–4f complex, well isolated from its congeners. Nevertheless complexes with three or four ions can also be useful if an alternate arrangement of the 3d and 4f ions is observed, without possible 3d–3d or 4f–4f interaction pathways. Until now, the most studied pair is Cu–Gd because

an isotropic Hamiltonian allows a straightforward determination of the J_{CuGd} magnetic interaction parameter.^{2–4} From the literature data it also appears that one of the most efficient bridges to transmit a magnetic interaction between Cu and Gd ions is the phenoxo bridge.⁵ Other di or trinuclear complexes associating Ni–Gd ions through phenoxo bridges are known, but we have to keep in mind that only high spin Ni ions are of interest,⁶ the low spin Ni ions being diamagnetic.⁷ The equivalent Mn^{II},⁸ Fe^{II},⁹ and Co^{II}¹⁰ complexes are more limited. Although Co^{II} ion is anisotropic and difficult to study from the magnetic point of view, it presents the advantage of having magnetically active high spin and low spin states, in comparison with the Ni^{II} or Fe^{II} ions that only have active high spin states. Some years ago, we prepared mixed amide–imine ligands able to coordinate Ni^{II}, Cu^{II}, or Mn^{III} complexes,¹¹ after deprotonation of three functions, two phenol and one amide functions. In the present paper, we describe the syntheses of the Co^{II} and Co^{II}–

Received: April 6, 2012

Published: May 23, 2012



Gd complexes, their X-ray structural determinations, and their magnetic studies. A preliminary communication concerning the low spin and square planar Co^{II} and Co^{II}–Gd complexes was previously published.¹²

EXPERIMENTAL SECTION

Materials. The metal salts, Co(CH₃COO)₂·4H₂O, Gd(NO₃)₃·5H₂O (Aldrich) were used as purchased. High-grade solvents were used for preparing the complexes. Gd(hfa)₃·2H₂O was prepared as previously described.¹³

Ligands. The syntheses of the different ligands were previously described,¹¹ starting from H₂L = *N*-(2-amino-2-methylpropyl)-2-hydroxybenzamide, H₂L' = *N*-(2-amino-propyl)-2-hydroxybenzamide or H₂L¹ = *N*-(3-amino-2,2-dimethylpropyl)-2-hydroxybenzamide (Scheme 2). In the present work, the trianionic ligands H₃L² = 2-hydroxy-*N*-(2-((1E)-(2-hydroxyphenyl)methylidene)amino)-2-methylpropyl)benzamide, H₃L^{2'} = 2-hydroxy-*N*-(2-((1E)-(2-hydroxyphenyl)methylidene)amino)-propyl)benzamide, H₃L^{2OMe} = 2-hydroxy-*N*-(2-((1E)-2-hydroxy-3-methoxyphenyl)methylidene)amino)-2-methylpropyl) benzamide, H₃L³ = 2-hydroxy-*N*-(3-((1E)-2-hydroxy-3-methoxyphenyl)methylidene)amino)-2,2-dimethylpropyl) benzamide are prepared in situ when synthesizing the metal complexes.

Complexes. The reactions and preparations of the samples for physical measurements were carried out in a purified nitrogen atmosphere within a glovebox (Vacuum Atmospheres H.E.43.2) equipped with a dry train (Jahan EVAC 7). The syntheses of the [L²Co]pipH (1) and [CoL²Gd(thd)₂(MeOH)]₂ (2) complexes were previously described.¹²

[L^{2OMe}Co(pipH)]_n (3). To a mixture of 0.5 mmol (104.0 mg) of H₂L and 0.5 mmol (76.0 mg) of *o*-vanillin in methanol (10 mL) was first added 0.5 mmol (125.0 mg) of Co(CH₃COO)₂·4H₂O and finally 1.5 mmol (127.0 mg) of piperidine. The reddish orange solution was stirred at room temperature for 30 min, filtered off, and left undisturbed. Reddish crystals appeared 10 days later. They were isolated and dried in the glovebox while the crystals used for X-ray diffraction (XRD) analysis were directly put in grease. Yield: 0.13 g (54%). Anal. Calcd for C₂₄H₃₁CoN₃O₄ (484.5): C, 59.5; H, 6.4; N, 8.7. Found: C, 58.8; H, 6.2; N, 8.3. IR data (ATR, cm⁻¹): 3045(w), 2966(m), 2945(w), 2926(w), 2859(w), 2840(w), 2725(w), 1638(m), 1618(m), 1591(s), 1559(m), 1528(m), 1510(m), 1465(m), 1426(s), 1436(s), 1385(vs), 1334(m), 1313(m), 1295(m), 1239(s), 1215(m), 1197(m), 1164(m), 1140(w), 1080(w), 1035(w), 983(m), 885(w), 852(w), 756(m), 742(m), 707(m), 654(w), 582(w). Vis (drs): 570, 750 nm.

[L^{2OMe}CoNa]_n (4). This complex was prepared as the previous complex by use of NaOH (60.0 mg, 1.5 mmol) instead of piperidine. It was isolated as a red powder by filtration and dried in the glovebox. Yield: 0.10 g (47%). Anal. Calcd for C₁₉H₁₉CoN₂NaO₄ (421.3): C, 54.2; H, 4.6; N, 6.6. Found: C, 53.8; H, 4.5; N, 6.2. IR data (ATR, cm⁻¹): 2963(w), 1600(m), 1564(s), 1502(vs), 1468(m), 1428(s), 1406(m), 1341(m), 1319(m), 1259(m), 1241(s), 1221(m), 1186(m), 1172(w), 1147(w), 1105(m), 992(w), 896(w), 866(w), 758(m), 731(m), 697(w), 659(w), 616(m). Vis (drs): 535, 710 nm.

[(pip)CoL^{2OMe}Gd(CH₃COO)(hfa)]₂ (5). To a mixture of 0.5 mmol (104.0 mg) of H₂L and 0.5 mmol (76.0 mg) of *o*-vanillin in methanol (10 mL) was first added 0.5 mmol (125.0 mg) of Co(CH₃COO)₂·4H₂O, 1.5 mmol (127.0 mg) of piperidine and finally 0.5 mmol (407.0 mg) of Gd(hfac)₃·2H₂O. The solution was stirred for 2 h and the yellowish orange precipitate formed was separated by filtration. The solution was left undisturbed and yellowish orange crystals of the same compound appeared 10 days later. Yield: 0.32 g (35%). Anal. Calcd for C₆₉H₆₈Co₂F₁₂Gd₂N₆O₁₆ (1813.6): C, 41.1; H, 3.8; N, 4.6. Found: C, 40.6; H, 3.4; N, 4.2. IR data (ATR, cm⁻¹): 3205(w), 2939(w), 1662(m), 1637(w), 1599(m), 1566(s), 1529(vs), 1504(m), 1462(m), 1437(m), 1389(m), 1287(w), 1248(s), 1194(s), 1142(vs), 1095(w), 953(w), 791(w), 759(w), 736(w), 710(w), 658(w). Vis (drs): 510, 810 nm.

[(CH₃OH)CoL^{2OMe}Gd(CH₃COO)(thd)]₂(MeOH)₂ (6). To a mixture of 0.5 mmol (104.0 mg) of H₂L and 0.5 mmol (76.0 mg) of *o*-vanillin in methanol (10 mL) was first added 0.5 mmol (125.0 mg) of Co(CH₃COO)₂·4H₂O, 1.5 mmol (127.0 mg) of piperidine, 0.5 mmol (188.0 g) of GdCl₃·6H₂O, and finally 1 mmol (0.184 g) of Hthd with 1 mmol (0.085 g) of piperidine. The solution was stirred for 2 h, and the yellowish orange precipitate was filtered off. The solution was left undisturbed, and yellowish orange crystals of the same compound appeared one month later. Yield: 0.20 g (23%). Anal. Calcd for C₆₈H₉₈Co₂Gd₂N₄O₂₀ (1723.9): C, 47.4; H, 5.7; N, 3.3. Found: C, 47.0; H, 5.5; N, 3.2. IR data (ATR, cm⁻¹): 3298(w), 2965(m), 1638(w), 1602(m), 1564(s), 1528(s), 1504(m), 1459(m), 1385(vs), 1356(m), 1244(m), 1224(m), 1142(w), 1098(w), 964(w), 868(w), 757(w), 736(m), 737(w). Vis (drs): 530, 750 nm.

[(thd)CoL³Gd(thd)]₂ (7). To a mixture of 0.5 mmol (111.0 mg) of H₂L¹ and 0.5 mmol (76.0 mg) of *o*-vanillin in methanol (10 mL) was first added 0.5 mmol (125.0 mg) of Co(CH₃COO)₂·4H₂O, 1.5 mmol (127.0 mg) of piperidine, 0.5 mmol (188.0 mg) of GdCl₃·6H₂O, and finally 1.5 mmol (276.0 mg) of Hthd with 1.5 mmol (127.0 mg) of piperidine. The solution was stirred for 2 h, and the dark green precipitate was filtered off. Yield: 0.30 g (53%). Anal. Calcd for C₁₀₆H₁₅₈Co₂Gd₂N₄O₂₀ (2240.8): C, 56.8; H, 7.1; N, 2.5. Found: C, 56.4; H, 6.9; N, 2.3. IR data (ATR, cm⁻¹): 2951(s), 2866(m), 1616(m), 1588(s), 1574(s), 1529(s), 1503(s), 1474(m), 1440(m), 1402(vs), 1386(s), 1356(s), 1241(m), 1219(m), 1177(w), 1138(m), 1077(w), 972(w), 868(w), 854(w), 792(w), 753(m), 736(m). Vis (drs): 510, 625, 940 nm.

[CoL²Gd(thd)₂(MeOH)]₂ (8). To a mixture of 0.5 mmol (97.0 mg) of H₂L' and 0.5 mmol (61.0 mg) of salicylaldehyde in methanol (10 mL) was first added 0.5 mmol (125.0 mg) of Co(CH₃COO)₂·4H₂O, 1.5 mmol (127.0 mg) of piperidine, 0.5 mmol (188.0 mg) of GdCl₃·6H₂O, and finally 1 mmol (184.0 mg) of Hthd with 1 mmol (85.0 mg) of piperidine. The solution was stirred for 2 h, and the orange precipitate was filtered off. The solution was left undisturbed and reddish orange crystals of the same compound appeared two weeks later. Yield: 0.30 g (65%). Anal. Calcd for C₈₀H₁₁₄Co₂Gd₂N₄O₁₆ (1820.2): C, 52.8; H, 6.3; N, 3.1. Found: C, 52.9; H, 6.5; N, 3.1. IR data (ATR, cm⁻¹): 3220(w), 2956(s), 1599(m), 1573(s), 1528(m), 1503(s), 1446(m), 1403(s), 1387(m), 1356(m), 1290(w), 1252(w), 1225(w), 1135(w), 1022(w), 869(w), 760(w). Vis (drs): 520 nm.

Physical Measurements. C, H, and N elemental analyses were carried out at the Laboratoire de Chimie de Coordination Micro-analytical Laboratory in Toulouse, France. IR spectra were recorded with a Perkin-Elmer Spectrum 100FTIR using the ATR mode. Diffuse reflectance spectra were recorded with a Perkin-Elmer Lambda 35 UV/vis spectrometer. Magnetic data were obtained with a Quantum Design MPMS SQUID susceptometer. Magnetic susceptibility measurements were performed in the 2–300 K temperature range under a 0.1 T applied magnetic field, and diamagnetic corrections were applied by using Pascal's constants.¹⁴ Isothermal magnetization measurements were performed up to 5 T at 2 K. The magnetic susceptibilities have been computed by exact calculations of the energy levels associated to the spin Hamiltonian through diagonalization of the full matrix with a general program for axial symmetry,¹⁵ and with the MAGPACK program package¹⁶ in the case of magnetization. Least-squares fittings were accomplished with an adapted version of the function-minimization program MINUIT.¹⁷

Crystallographic Data Collection and Structure Determination for the Complexes 3, 5, 6. Crystals of 3, 5, and 6 were kept in the mother liquor until they were dipped into oil. The chosen crystals were mounted on a Mitegen micromount and quickly cooled down to 180 or 150 K. The selected crystals of 3 (orange, 0.25 × 0.18 × 0.07 mm³), 5 (yellowish orange, 0.18 × 0.13 × 0.08 mm³), 6 (yellowish orange, 0.22 × 0.12 × 0.03 mm³) were mounted on an Oxford-Diffraction XCALIBUR (3, 5, 6) using a graphite monochromator (λ = 0.71073 Å) and equipped with an Oxford Cryosystems cooler device. The data were collected at 180 K. The unit cell determination and data integration were carried out using the CrysAlis RED package for the data recorded on the Xcalibur package.¹⁸ A total of 15716 reflections were collected for 3, of which 4480 were

Table 1. Crystallographic Data for Complexes $[(L^{2OMe}Co)pipH]_n$ (3), $[(pip)CoL^{2OMe}Gd(CH_3COO)(hfa)]_2$ (5), and $[(CH_3OH)CoL^{2OMe}Gd(CH_3COO)(thd)]_2$ (6)

	3	5	6
formula	$C_{24}H_{31}CoN_3O_4$	$C_{62}H_{68}Co_2F_{12}Gd_2N_6O_{16}$	$C_{68}H_{98}Co_2Gd_2N_4O_{20}$
Fw	484.45	1813.58	1723.85
space group	$P2_1/c$	$P2_1/n$	$P2_1/c$
<i>a</i> , Å	10.4005(10)	12.7513(2)	14.8669(2)
<i>b</i> , Å	9.2090(7)	15.7355(2)	13.8521(2)
<i>c</i> , Å	23.2616(18)	17.8631(3)	18.595(3)
α , deg	90	90	90
β , deg	100.273(8)	104.231(2)	104.405(2)
γ , deg	90	90	90
<i>V</i> , Å ³	2192.2(3)	3474.21(9)	3709.1(6)
<i>Z</i>	4	2	2
ρ_{calcd} , g cm ⁻³	1.468	1.734	1.542
λ , Å	0.71073	0.71073	0.71073
<i>T</i> , K	180(2)	180(2)	180(2)
μ (Mo K α), mm ⁻¹	0.820	2.454	2.275
<i>R</i> ^a obs, all	0.1857, 0.2185	0.0278, 0.0432	0.0204, 0.0297
<i>wR</i> ^b obs, all	0.4127, 0.4285	0.0619, 0.0643	0.0469, 0.0480

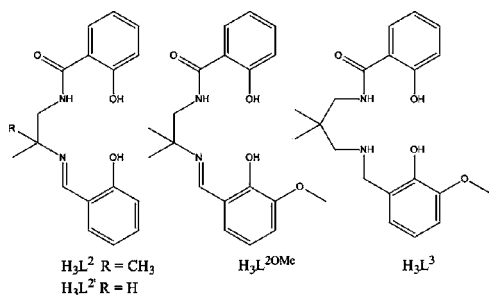
$$^a R = \sum \|F_o\| - \|F_c\| / \sum \|F_o\|, \quad ^b wR_2 = [\sum w(F_o^{21} - F_c^{21})^2 / \sum wF_o^{21}]^{1/2}.$$

independent ($R_{\text{int}} = 0.1220$), 36165 reflections for 5, of which 7083 were independent ($R_{\text{int}} = 0.0349$), 31517 reflections for 6, of which 7563 were independent ($R_{\text{int}} = 0.0304$). The structures have been solved by Direct Methods using SIR92,¹⁹ and refined by least-squares procedures on F^2 with the program SHELXL97²⁰ included in the software package WinGX version 1.63.²¹ Atomic Scattering Factors were taken from the International tables for X-ray Crystallography.²² All hydrogen atoms were geometrically placed and refined by using a riding model. All non-hydrogen atoms were anisotropically refined, and in the last cycles of refinement a weighting scheme was used, where weights are calculated from the following formula: $w = 1/[\sigma^2(F_o^2) + (aP)^2 + bP]$ where $P = (F_o^2 + 2F_c^2)/3$. Drawings of molecules are performed with the program ORTEP32²³ with 30% probability displacement ellipsoids for non-hydrogen atoms. Crystal data collection and refinement parameters are given in Table 1.

RESULTS

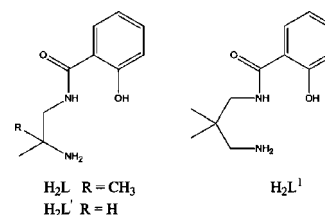
The ligands used in the present work appear in Scheme 1. Their synthesis requires a stepwise process. Reaction of phenyl

Scheme 1



salicylate with the different diamines in propane-2-ol first produces the amide part of the ligands (Scheme 2). Then reaction of the primary amine function of these different half-unit ligands with salicylaldehyde or *o*-vanillin yields the desired ligands reported in Scheme 1. With the H_3L^2 ligand, the mononuclear complex $[(L^2Co)(pipH)]$ (1) and the tetranuclear compound $[CoL^2Gd(thd)_2(MeOH)]_2$ (2) were obtained, both previously described in a short communication.¹² The use of the H_3L^{2OMe} ligand with the same experimental procedure

Scheme 2



allowed to isolate the one-dimensional (1D) complex $[(L^{2OMe}Co)(pipH)]_n$ (3) while replacement of piperidine by NaOH yielded also another 1D system $[L^{2OMe}CoNa]_n$ complex (4). Addition of $Gd(hfa)_3 \cdot 2H_2O$ to the solution giving (3) yielded the tetranuclear $[(pip)CoL^{2OMe}Gd(CH_3COO)(hfa)]_2$ complex (5) as orange crystals while addition of $GdCl_3 \cdot 6H_2O$, tetramethylheptanedione (Hthd), and piperidine (1:2:3 ratio) to the solution giving (4) yielded the tetranuclear $[(CH_3OH)CoL^{2OMe}Gd(CH_3COO)(thd)]_2$ complex (6), as orange crystals. A similar experimental pathway with the H_3L^3 ligand gave again yellow green crystals corresponding to a tetranuclear complex formulated as $[(thd)CoL^3Gd(thd)_2]_2$ (7) while for the $H_3L^{2'}$ ligand, a tetranuclear compound $[CoL^{2'}Gd(thd)_2(MeOH)]$ (8) was obtained as reddish orange crystals. The entire set of complexes were prepared in a glovebox but once isolated and dried, the crystals of complexes (1–3, 5–8) are stable in the open atmosphere. The presence of ligand is evidenced by several intense bands in the IR spectra. The bands around 1600 cm⁻¹ correspond to the stretching vibrations of the deprotonated amide functions while the large bands in the 2800–2400 cm⁻¹ region do correspond to the piperidinium cation. It is easier to assign C=O (1662 cm⁻¹) and C–F stretching vibrations (1248–1142 cm⁻¹) coming from hefluoroacetylacetonato (hfa) than the C=O bands from tetramethylheptanedionato (thd) auxiliary ligands. This last ligand is better characterized by the strong C–H stretching vibrations around 2950–2960 cm⁻¹. As we could not obtain a structural determination with the isolated crystals of complex 8, confirmation of the square planar environment was given by diffuse reflectance spectra. Indeed, the weak band appearing in

the 650–800 nm region with five coordinate and high spin Co ions, is not present in the spectra of square planar low spin Co ions.

Description of the Structures. The descriptions of complexes **1** and **2**, which have been previously published, are not reported here. A view of these complexes is given in the Supporting Information, Figures S1 and S2. The structures of complexes **3**, **5**, **6**, and **7** were determined by single-crystal X-ray diffraction. The structure of **3** consists of a 1D system made of a chain of anionic $L^{2OMe}Co^-$ units and piperidinium cations, with the Co^{II} ion located in the N_2O_2 site of the triply deprotonated L^{2OMe} ligand (Figure 1). We are aware about the

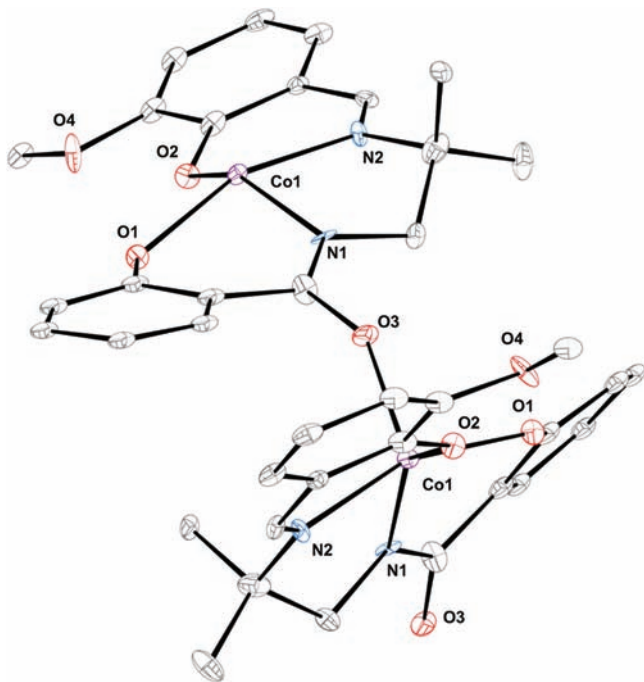


Figure 1. Partial view of the 1D chain for complex **3**.

poor quality of the compound **3** structure. Performing a PLATON ADSYM TEST confirmed the retained space group ($P2_1/c$) while running ROTAX in CRYSTAL proposed several twin laws. We are dealing with a poly crystal, which explains the high R1 factor, the high electron density minimum, and some bad ellipsoids. The Co ion deviates by 0.501(2) Å from the mean coordination plane defined by the four donor atoms, contrary to complex **1** where the Co ion is practically in the mean coordination plane.¹² This difference is due to the cobalt environment, which is square planar in complex **1** and square pyramidal in complex **3**, the axial position being occupied by the oxygen atom of the deprotonated amide function of the next $L^{2OMe}Co^-$ entity. Such an arrangement yields a 1D chain made of $L^{2OMe}Co$ units with two different orientations (Figure 1). The mean coordination N_2O_2 planes of these two units make a dihedral angle of 41.4(3)°. The distance between the two next Co ions is equal to 5.916(3) Å while the distance between the two Co ions having the same orientation is 9.209(3) Å. Formation of the chain induces a larger deformation of the L^{2OMe} ligand. So the dihedral angle between the two benzene rings equals 19.8(5)° in **3**, in contrast to the value of 3.87(7)° found in **1**. The five-membered cycle implying the diamino chain is in a δ gauche conformation in one chain and λ gauche in the next one. The Co–N (2.00(1)

and 2.12(1) Å) and Co–O bond lengths (2.002(9) and 2.07(1) Å) are longer than the equivalent bonds in complex **1**, as expected in going from a square planar to a square pyramidal cobalt environment. The shorter bond is the axial bond implying the oxygen amide atom (Co–O4 = 1.99(1)Å). The piperidinium cation is hydrogen-bonded to the two phenoxo and to the methoxy oxygen atoms of the L^{2OMe} ligand. Although of poor quality, this structural determination does confirm that **3** is a 1D system with pentacoordinate cobalt ions.

In complex **6** two heteronuclear Co–Gd entities are assembled through the oxygen atoms of the amide groups to form a double (Co–N–C–O–Gd) bridge leading to a tetranuclear entity, as represented in Figure 2. In each Co–

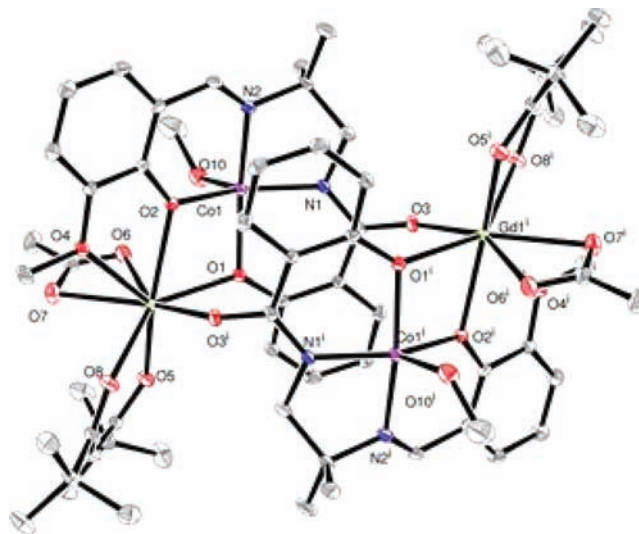


Figure 2. View of the tetranuclear $[Co-Gd]_2$ complex **6**. Selected bond lengths (Å) and angles (deg): Co N1 1.964(2), Co N2 2.064(2), Co O1 2.047(2), Co O2 1.972(2), Co O10 2.079(2), Gd O1 2.383(2), Gd O2 2.387(1), Gd O3 2.278(2), Gd O4 2.559(2), Gd O5 2.310(2), Gd O6 2.489(2), Gd O7 2.514(2), Gd O8 2.320(2), O1 Co O2 84.28(6), O1 Gd O2 68.87(5), Co O1 Gd 101.95(6), Co O2 Gd 104.14(6).

Gd unit, the cobalt ion is again in the inner N_2O_2 site, deviating by 0.475(3) Å from the mean N_2O_2 coordination plane. The axial position of the square pyramidal coordination is occupied by the oxygen atom of a MeOH molecule, in place of the oxygen amide atom, now involved in the Co–N–C–O–Gd bridge. The cobalt ion is doubly bridged by two phenoxo oxygen atoms to the gadolinium ion. This Co–(O)₂–Gd bridging network is not planar since the dihedral angle between the (OCoO) and (OGdO) planes is equal to 8.3(1)°, thus giving a Co–Gd distance of 3.4474(3) Å. The five-membered cycle of the two ligands forming the tetranuclear unit are respectively in δ gauche and λ gauche conformations. The gadolinium ion is eight coordinate; in addition to the two bridging phenoxo oxygen and the methoxy oxygen atoms of the L^{2OMe} ligand, four oxygen atoms coming from the bidentate η^2 -coordinated thd diketone ligand and from the chelating acetate ligand, while the amide oxygen not involved in the Co coordination site complete its environment. The Gd–O bond lengths vary from 2.278(2) to 2.514(2) Å, depending on the nature of the oxygen atoms. Inside the tetranuclear complex, the Co...Co and Gd...Gd distances are equal to 6.747(3) and 7.842(4) Å, respectively. It has to be noted that the MeOH linked to the Co ion and the acetate chelating the Gd ion are

located on the outer face of the tetranuclear unit, thus impeding formation of intermolecular hydrogen bonds. The two oxygen atoms of the acetate ligand make intramolecular hydrogen bonds with the coordinated MeOH molecule for one oxygen and the non coordinated MeOH molecule for the other. So these tetranuclear entities are well isolated from each other, the shortest intermolecular Gd...Gd distances being larger than 10 Å, precluding any significant interaction of magnetic nature between these tetranuclear units. A comparison with complex 3 indicates that the basal Co–N (1.964(2) and 2.065(2) instead of 2.00(1) and 2.12(1) Å) and Co–O (1.972(2) and 2.047(2) instead of 2.002(9) and 2.07(1) Å) bond lengths are shorter in complex 6 while the apical Co–O bond is longer (2.079(2) instead of 1.99(1) Å). But these Co–N and Co–O bond lengths are larger than those of the tetranuclear complex 2 having low spin and square planar Co ions.

Complex 5 is also a tetranuclear entity in which two heteronuclear Co–Gd entities are assembled through the oxygen atoms of the amide groups (Figure 3). It is made with

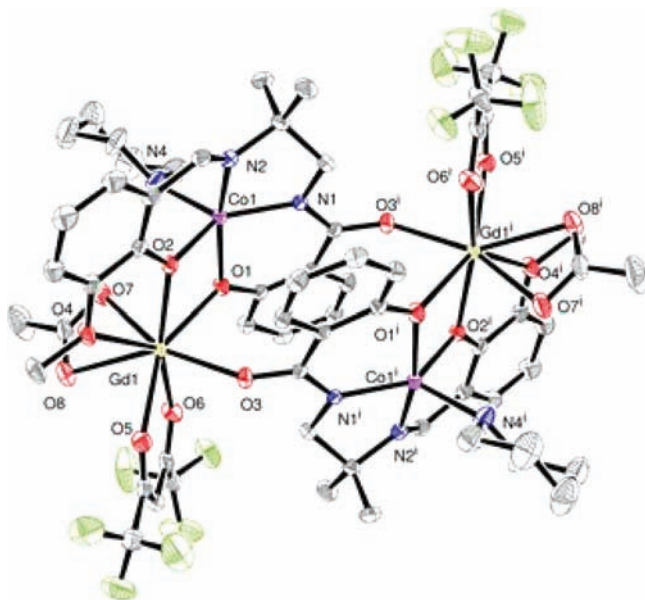


Figure 3. View of the tetranuclear $[\text{Co-Gd}]_2$ complex 5. Selected bond lengths (Å) and angles (deg): Co N1 1.973(2), Co N2 2.061(3), Co N4 2.093(3), Co O1 2.050(2), Co O2 1.988(2), Gd O1 2.359(2), Gd O2 2.331(2), Gd O3 2.267(2), Gd O4 2.550(2), Gd O5 2.394(2), Gd O6 2.373(2), Gd O7 2.402(3), Gd O8 2.492(2), O1 Co O2 83.79(8), O1 Gd O2 70.18(7), Co O1 Gd 101.42(8), Co O2 Gd 104.35(8).

the same amide-imine main ligand $L^{2\text{OMe}}$ and an acetate ligand chelates again the gadolinium ion. In comparison to complex 6, two different ancillary ligands are present: the thd diketone chelating the Gd ion is replaced by deprotonated hexafluoroacetylacetonate (hfa) while the nitrogen atom of piperidine occupies the cobalt axial position in place of the oxygen atom of a methanol molecule. The geometrical parameters of the two complexes are quite similar, particularly the Co–N and Co–O bond lengths, and the dihedral angle between the (OCoo) and (OGdO) planes is now equal to $4.9(1)^\circ$, giving a Co–Gd distance of 3.4181(4) Å. An oxygen atom of the acetate ligand makes an intramolecular hydrogen-bond with the Co coordinated piperidine nitrogen atom in complex 5. A SHAPE analysis confirms that the Co coordination spheres in

complexes 3, 5, and 6 correspond to distorted square pyramids ($S_{\text{py}} = 1.14, 1.88, 1.52$ respectively).²⁴

Because of the poor quality of crystals, the structural determination for complex 7 could not be refined to an adequate standard. Nevertheless several observations that are not subject to controversy can be done, the high R factor being due to the disorder introduced by the methyl groups of the ancillary thd ligands. A view of the tetranuclear $[\text{Co-Gd}]_2$ complex 7 (Supporting Information, Figure S4) confirms that we are again dealing with a tetranuclear complex, different from the two previous tetranuclear complexes 5 and 6. The main difference comes from the fact that the Co ion is not wrapped around the N_2O_2 coordination site of the ligand since the amide function is not deprotonated. As the ligand is dianionic, with its two deprotonated phenol functions, three supplementary anionic charges, brought by three ancillary thd ligands, are needed. The Co ion is linked to the imine nitrogen atom and the oxygen atom coming from the *o*-vanillin part of the ligand and to the deprotonated phenol function located near the amide function of a second ligand. Its five coordination environment is completed by the two oxygen atoms of a thd ancillary ligand. The Gd ion is linked to the *o*-vanillin part of the main ligand by its phenoxo and methoxy oxygen atoms and to the oxygen amide and phenol atoms of the second ligand, its eight coordination sphere being completed by four oxygen atoms from two thd ancillary ligands. The Co and Gd ions are assembled by a double phenoxo bridge, and the tetranuclear complex is made of two independent Co–Gd pairs. It is also clear that there are two different tetranuclear units in the unit cell, which is due to the helicity of the two pentacoordinated Co ions that present a Δ helicity in one unit while they have a Λ helicity in the other one. The SHAPE analysis²⁴ indicates that the Co geometry is best described as trigonal bipyramid, with S_{TBPY} parameters equal to 1.98, 1.44, 1.30, 1.47 for Co₁, Co₂, Co₃, and Co₄ ions, respectively. There are again no intermolecular hydrogen bonds between adjacent tetranuclear units of 7, and the shorter Co...Co intermolecular distances are larger than 8 Å, as in complexes 5 and 6.

Magnetic Properties. The magnetic susceptibility of the 1D complex 3, measured in the 2–300 K temperature range under an applied magnetic field of 0.1 T, is displayed in Figure 4. The $\chi_{\text{M}}T$ value, equal to $2.60 \text{ cm}^3 \text{ mol}^{-1} \text{ K}$ at room

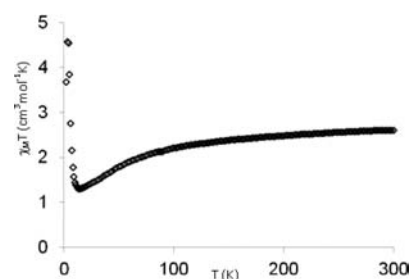


Figure 4. Temperature dependence of the $\chi_{\text{M}}T$ product for complex 3 at 0.1 T applied magnetic field.

temperature, which is practically constant down to 100 K, slowly decreases from 100 to 14 K ($1.30 \text{ cm}^3 \text{ mol}^{-1} \text{ K}$), then increases sharply to $4.57 \text{ cm}^3 \text{ mol}^{-1} \text{ K}$ at 3 K before decreasing again to $3.67 \text{ cm}^3 \text{ mol}^{-1} \text{ K}$ at 2 K. From the room temperature $\chi_{\text{M}}T$ value, it is clear that the Co ions are in a high spin state ($\mu = 4.56 \mu_{\text{B}}$), and the sharp $\chi_{\text{M}}T$ increase suggests the onset of a ferromagnetic order. To confirm the magnetic phase transition,

alternating current (ac) susceptibility measurements have been investigated on complex 3. These ac susceptibility measurements show in-phase and out-of-phase signals. Unfortunately we cannot see the χ'' maxima, even at 2 K, but the shape of the χ'' curve at different frequencies, 800, 1000, and 1200 Hz (Supporting Information, Figure S5), confirms that these signals are not frequency-dependent. In view of the structure, such a behavior is characteristic of a two-dimensional weak ferromagnetic ordering. In the case of complex 4, the room temperature $\chi_M T$ value is consistent with Co ions in a high spin state ($\mu = 4.21 \mu_B$), and the $\chi_M T$ increase at low temperature, although weaker, is also observed (Supporting Information, Figure S6).

The magnetic susceptibilities of the tetranuclear [Co–Gd]₂ complexes 5–7 have been measured in the 2–300 K temperature range under an applied magnetic field of 0.1 T. Complex 7, with two well separated Co–Gd pairs, will be examined first for it represents the simpler example. The thermal variation of the $\chi_M T$ product for complex 7 is displayed in Figure 5. As the structure shows two magnetic independent

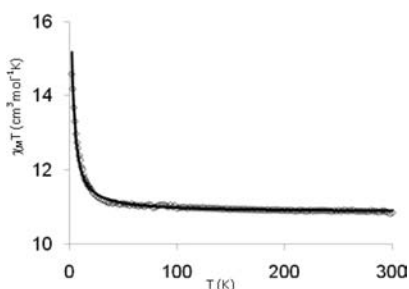


Figure 5. Temperature dependence of the $\chi_M T$ product for complex 7 at 0.1 T applied magnetic field. The solid line corresponds to the best data fit: $J_{\text{Co-Gd}} = 0.40 \text{ cm}^{-1}$, $g = 2.11$.

dinuclear units, the magnetic data are referred only to one dinuclear entity. At 300 K, $\chi_M T$ is equal to $10.90 \text{ cm}^3 \text{ mol}^{-1} \text{ K}$ which is larger than the value expected for uncoupled cobalt and gadolinium ions with $g = 2$ ($9.75 \text{ cm}^3 \text{ mol}^{-1} \text{ K}$). This difference is easily explained if we remember that an orbital contribution from the Co ion is present. Lowering the temperature results in a slow $\chi_M T$ increase down to 20 K ($11.48 \text{ cm}^3 \text{ mol}^{-1} \text{ K}$) and then in a more abrupt one, up to $14.6 \text{ cm}^3 \text{ mol}^{-1} \text{ K}$ at 2 K. This behavior indicates that a ferromagnetic interaction between the Co^{II} ($S = 3/2$) and Gd^{III} ($S = 7/2$) ions operates at low temperature. Because of the orbital degeneracy of high-spin cobalt(II) ($S = 3/2$), interpretation of the data by using an isotropic spin Hamiltonian is not rigorous in the case of complex 7. Nevertheless, because of the presence of an isotropic Gd ion, we have tried to check if an isotropic Hamiltonian taking into account the Co–Gd interaction could give a rough estimation of the interaction parameter. The magnetic susceptibility has been computed by exact calculation of the energy levels associated with the spin Hamiltonian through diagonalization of the full E-matrix. The best fit yields a $J_{\text{Co-Gd}}$ value of 0.40 cm^{-1} ($H = -J_{\text{Co-Gd}} S_{\text{Co}} S_{\text{Gd}}$) with $g = 2.11$ and an agreement factor $R = \sum [(\chi_M T)_{\text{obs}} - (\chi_M T)_{\text{calc}}]^2 / \sum [(\chi_M T)_{\text{obs}}]^2$ equal to 3×10^{-5} .

As the complexes 5 and 6 have similar structures and as a consequence similar magnetic behaviors, the thermal variation of the $\chi_M T$ product for complex 6 is reported in Figure 6 while that of complex 5 appears in Supporting Information, Figure

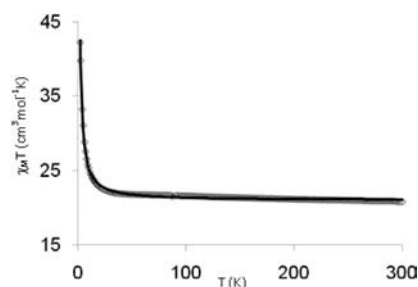


Figure 6. Temperature dependence of the $\chi_M T$ product for complex 6 at 0.1 T applied magnetic field. The solid line corresponds to the best data fit: $J_{\text{Co-Gd}} = 0.40 \text{ cm}^{-1}$, $j_{\text{Co-Gd}} = 0.24 \text{ cm}^{-1}$, $D_{\text{Co}} = 1.6 \text{ cm}^{-1}$, $g = 2.07$.

S7. At 300 K, the $\chi_M T$ product for the tetranuclear unit is equal to $20.9 \text{ cm}^3 \text{ mol}^{-1} \text{ K}$. Upon lowering the temperature, $\chi_M T$ slowly increases to $22.9 \text{ cm}^3 \text{ mol}^{-1} \text{ K}$ at 20 K, and then sharply to $42.2 \text{ cm}^3 \text{ mol}^{-1} \text{ K}$ at 2 K, indicating again the presence of a ferromagnetic interaction. The energy levels and magnetic properties of spin systems including anisotropic cobalt(II) ion usually require consideration of single ion ZFS terms. This ZFS term includes the anisotropy originating from the orbital contribution. The simpler spin Hamiltonian that may be used is $H = -J_{\text{Co-Gd}}(S_{\text{Co1}} S_{\text{Gd1}} + S_{\text{Co2}} S_{\text{Gd2}}) - j_{\text{Co-Gd}}(S_{\text{Co1}} S_{\text{Gd2}} + S_{\text{Co2}} S_{\text{Gd1}}) + 2D_{\text{Co}} S_z^2 S_{\text{Co}} + \sum_{ij} g_i \beta H_i S_{ij}$ in which the first two terms gauged by the J and j parameters account for the spin exchange interaction through respectively the double phenoxo and single amido bridges, the third one gauged by D accounts for axial single ion ZFS of cobalt(II) and the fourth one accounts for the Zeeman contributions where $i = \text{Co}, \text{Gd}$ and $j = x, y, z$. The temperature dependence of $\chi_M T$ was fitted using the above Hamiltonian. The best fit for complex 6 (Figure 6) was obtained for the following set of parameters, $J_{\text{Co-Gd}} = 0.40 \text{ cm}^{-1}$, $j_{\text{Co-Gd}} = 0.24 \text{ cm}^{-1}$, $D_{\text{Co}} = 1.6 \text{ cm}^{-1}$, $g = 2.07$, $R = 7 \times 10^{-5}$. Complex 5 gives $J_{\text{Co-Gd}} = 0.28 \text{ cm}^{-1}$, $j_{\text{Co-Gd}} = 0.26 \text{ cm}^{-1}$, $D_{\text{Co}} = -0.45 \text{ cm}^{-1}$, $g = 2.08$, $R = 1 \times 10^{-4}$ (Supporting Information, Figure S7). It is interesting to note that the two interaction constants, through the double phenoxo bridge and through the single amido bridge, are ferromagnetic. In view of the previous result obtained with complex 7, the larger $J_{\text{Co-Gd}}$ value must be attributed to the double phenoxo bridge. On the contrary, we cannot concede a great interest to the ZFS Co parameters. Surprisingly, application of the above Hamiltonian including ZFS terms did not give better results for complex 7.

The $\chi_M T$ product reported in Figure 7 for compound 8 is equal to $16.9 \text{ cm}^3 \text{ mol}^{-1} \text{ K}$ at 300 K. From 100 to 50 K, a slight

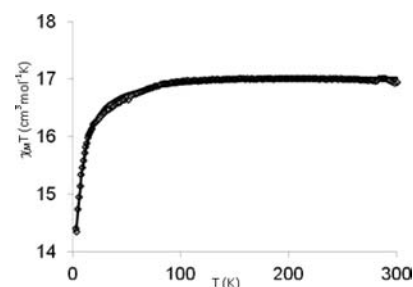


Figure 7. Temperature dependence of the $\chi_M T$ product for the tetranuclear complex 8 at 0.1 T applied magnetic field. The solid line corresponds to the best data fit: $J_{\text{Co-Gd}} = -1.27 \text{ cm}^{-1}$, $j_{\text{Co-Gd}} = -0.24 \text{ cm}^{-1}$, $g = 2.04$.

decrease to $16.7 \text{ cm}^3 \text{ mol}^{-1} \text{ K}$ is observed, followed by a sharp decrease until $14.4 \text{ cm}^3 \text{ mol}^{-1} \text{ K}$ at 2 K. The $\chi_M T$ at room temperature is slightly larger than expected for two isolated Co and two Gd ions ($16.5 \text{ cm}^3 \text{ mol}^{-1} \text{ K}$) with $g = 2$ but it evidence that the cobalt ion is still in a low spin state. The experimental data indicate the occurrence of an overall antiferromagnetic interaction in complex **8**. The magnetic susceptibility has been computed by exact calculation of the energy levels associated with the above spin Hamiltonian without the ZFS term, through diagonalization of the full energy-matrix. The best fit yields the following data, $J_{\text{Co-Gd}} = -1.27 \text{ cm}^{-1}$, $j_{\text{Co-Gd}} = -0.24 \text{ cm}^{-1}$, $g = 2.04$, with a R factor equal to 6.0×10^{-5} . To check the validity of these results, the Magpack program has been used to fit the experimental magnetization curve at low temperature.¹⁶ The $J_{\text{Co-Gd}}$ value appears to be slightly overestimated for the 2–5 T part of the curve. A much better fit of magnetization is obtained with a lower $J_{\text{Co-Gd}}$ value, -0.90 cm^{-1} associated to a zero $j_{\text{Co-Gd}}$ value (Supporting Information, Figure S8). A similar remark was previously put forward for complex **2**, consistent with an overestimation of the $j_{\text{Co-Gd}}$ interaction through the amido bridge in complexes **2** and **8**. A new fit of the $\chi_M T$ product for compound **8** with these parameters gives a satisfactory result (Supporting Information, Figure S9).

DISCUSSION

To facilitate discussion, a view of the previously published tetranuclear $[\text{Co-Gd}]_2$ in which the Co ions are in a square planar coordination sphere, is given in the Supporting Information, Figure S2, along with the temperature dependence of its $\chi_M T$ product (Supporting Information, Figure S10). The main interest of the present work consists in showing that use of trianionic amide-imine ligands differing only by a methoxy group (H_3L^2 and $\text{H}_3\text{L}^{2\text{OMe}}$ ligands in Scheme 1) not involved in the coordination site of the Co^{II} ions can yield anionic Co complexes with Co ions in high spin ($S = 3/2$) or low spin ($S = 1/2$) states. In the low spin state, the Co^{II} ions are in a square planar environment (complex **1**) while they are in a square pyramid environment in the high spin state (complexes **3**, **4**). Furthermore these Co spin states and coordination spheres are preserved when Gd ions are introduced in these $[\text{LCo}]^-$ units to give eventually tetranuclear $[\text{LCo-Gd}]_2$ complexes with ancillary ligands chelated to the Gd ions. The head to tail arrangement of two LCo-Gd units gives a tetranuclear complex in which the Co and Gd ions are alternately bridged through a double phenoxo bridge or a single amido bridge. Surprisingly, these tetranuclear complexes are governed by opposite magnetic behaviors. Antiferromagnetic $J_{\text{Co-Gd}}$ interactions are active in complexes involving low spin Co ions while ferromagnetic $J_{\text{Co-Gd}}$ interactions characterize complexes containing high spin Co ions. Such an experimental observation should be rich information for the understanding of the mechanism governing the magnetic interaction in 3d-Gd entities. Indeed in the low spin Co ions, seven electrons are located in four 3d orbitals, the in plane e_g orbital of the $d_{x^2-y^2}$ type being unoccupied. In the high spin Co ions, five electrons are in the t_{2g} orbitals while the two remaining electrons are in the two singly occupied e_g orbitals, whatever the geometry, deformed square based pyramid or deformed trigonal bipyramid. So the single occupation of the $d_{x^2-y^2}$ orbital or its vacancy should be responsible for the change of the magnetic behavior.

In copper–gadolinium complexes, we have previously shown that the interaction parameter J_{CuGd} was a function of the CuO_2Gd dihedral angle defined as the angle between the OCuO and OGdO planes of the central CuO_2Gd core, O_2 representing the two phenoxo bridges.⁵ Deviation from planarity reduces the ferromagnetic interaction. In the Cu–Gd complexes with a double phenoxo bridge, J_{CuGd} goes from 10.1 cm^{-1} for a practically planar CuO_2Gd core ($1.7(2)^\circ$)⁵ to 0.2 cm^{-1} for a dihedral angle equal to $41.6(2)^\circ$.²⁵ Although the interaction tends to zero with large dihedral angles, it remains ferromagnetic. So in our $[\text{Co-Gd}]_2$ complex with square planar Co ions, which is characterized by a large dihedral angle equal to $41.6(1)^\circ$, we should expect a very weak ferromagnetic $J_{\text{Co-Gd}}$ parameter. The presence of an antiferromagnetic $J_{\text{Co-Gd}}$ parameter, that cannot be related to the dihedral angle, must be associated to the depopulation of the $d_{x^2-y^2}$ orbital.

A look at literature data also gives a convincing argument. Till now, all the Cu–Gd complexes involving double phenoxo bridges display ferromagnetic interactions.^{1–5,25} Even single three-atom bridges linking the Cu and Gd ions, as in the Cu–N–C–O–Gd bridge, do yield ferromagnetic J_{CuGd} interactions.²⁶ The few Cu–Gd examples in which an antiferromagnetic interaction was detected do involve the oxime bridge.²⁷ As this two-atom bridge gives Cu–Gd complexes that behave in a different way,²⁸ we have not taken into consideration in our analysis the complexes associating copper to gadolinium through an oxime bridge. When double or triple phenoxo bridges link gadolinium to Ni^{II} ,⁶ Co^{II} ,¹⁰ Fe^{II} ,⁹ or Mn^{II} ions,⁸ ferromagnetic interactions are present. In all of these examples the $3d_{x^2-y^2}$ orbitals are singly occupied. In the case of Cr^{III} complexes the $d_{x^2-y^2}$ orbital is unoccupied; unfortunately there is no example of Cr^{III} –Gd complex with phenoxo bridges, but complexes with single Cr–F–Gd fluoro²⁹ or oxalato³⁰ bridges are always characterized by antiferromagnetic J_{CrGd} interactions. It has to be noted that the Cr–Dy interaction in an octanuclear $\text{Cr}^{\text{III}}_4\text{Dy}^{\text{III}}_4$ entity with alkoxo and hydroxo Cr–O–Dy bridges has been found antiferromagnetic in ab initio calculations.³¹ Mn^{III} ions have been often associated with Dy ions to yield SMMs, but there are few examples of complexes associating Mn^{III} and Gd ions.³² Even in the simplest cases,^{32c,e,f} there is no proof for the presence of ferromagnetic Mn^{III} –Gd interactions. On the contrary a dinuclear Fe^{III} –Gd complex associating a high spin Fe^{III} ion and Gd^{III} with a triple phenoxo bridge shows a ferromagnetic interaction.³³ The cyano-bridged coordination polymers have been reviewed and a study of their magnetic properties indicates that the Gd– Fe^{III} (low spin) and Gd– Cr^{III} interactions are antiferromagnetic.⁴ Very recently, it has been shown that a double O–C–N bridge associating a low spin Fe^{III} (with unoccupied $3d_{x^2-y^2}$ orbital) to a Gd ion gives an antiferromagnetic interaction.³⁴ From this literature review of complexes associating transition metal ions from Cr^{III} to Cu^{II} with Gd^{III} ions, it appears that ferromagnetic interactions are found when the $3d_{x^2-y^2}$ orbital of the transition metal is singly occupied while antiferromagnetic interactions do characterize the complexes with unoccupied transition metal $3d_{x^2-y^2}$ orbitals, in complete agreement with our present experimental observation in the complexes assembling high spin or low spin Co^{II} with Gd^{III} ions. This observation has to be brought together with a previous rule of thumb that associated the deviation from planarity of the CuO_2Gd core to a decrease of the ferromagnetic interaction.⁵ Although the mechanism of the 3d-Gd magnetic interaction has been the subject of recent and interesting developments,^{34,35} it seems dangerous and risky to

give an interpretation of the present experimental results without support of theoretical results.

CONCLUSION

The main interest of the present work consists in showing that use of trianionic amide-imine ligands differing only by a methoxy group (H_3L^2 and H_3L^{2OMe} ligands in Scheme 1) not involved in the coordination site of the Co^{II} ions can yield anionic Co complexes with Co ions in high spin ($S = 3/2$) or low spin ($S = 1/2$) states. In the low spin state, the Co^{II} ions are in a square planar environment while they are in a square pyramid environment in the high spin state. Introduction of Gd ions in presence of ancillary ligands chelating the Gd ions yields tetranuclear complexes in which the Co and Gd ions are alternately bridged through a double phenoxo bridge or a single amido bridge, as a consequence of the head to tail arrangement of two LCo-Gd units. It is interesting to note that these Co spin states and coordination spheres are preserved in going from the Co^{II} complexes to the heterometallic species. As the ancillary ligands enter mainly in the Gd coordination sphere, they do not modify the Co^{II} spin states. In a previous work, we have shown that deviation from planarity of the CuO_2Gd core was associated with a decrease of the ferromagnetic interaction. Now, with help of the Co-Gd complexes, we can better understand our observation for the Co^{II} ions present the huge advantage of having magnetically active high spin and low spin states. We have shown that ferromagnetic interactions are found when the Co^{II} $d_{x^2-y^2}$ orbital is singly occupied while antiferromagnetic interactions do characterize the complexes with unoccupied Co^{II} $3d_{x^2-y^2}$ orbitals. To confirm this experimental observation, a look at literature data confirms that antiferromagnetic interactions are found in the 3d-Gd complexes ($3d = Cr^{III}, Mn^{III},$ low spin Fe^{III}) with unoccupied $3d_{x^2-y^2}$ orbitals, in complete agreement with our experiments.

ASSOCIATED CONTENT

Supporting Information

Crystallographic data in CIF format. Further details are given in Figures S1–S10. This material is available free of charge via the Internet at <http://pubs.acs.org>.

AUTHOR INFORMATION

Corresponding Author

*E-mail: jean-pierre.costes@lcc-toulouse.fr.

Notes

The authors declare no competing financial interest.

ACKNOWLEDGMENTS

This work was supported by CNRS, MAGMANet (Grant NMP3-CT-2005-515767), the Ministerio de Ciencia e Innovación of Spain through the project CTQ2009-07264/BQU and the Comissio Interdepartamental de Recerca I Innovacio Tecnologica de la Generalitat de Catalunya CIRIT (2009-SGR1454). V.G. is grateful to the Ministerio de Ciencia e Innovación for the Ph.D. Grant BES-2007-15668. The authors are grateful to Dr. A. Mari for technical assistance.

REFERENCES

- (1) Sessoli, R.; Powell, A. K. *Coord. Chem. Rev.* **2009**, *253*, 2328–2341.
- (2) Benelli, C.; Gatteschi, D. *Chem. Rev.* **2002**, *102*, 2369–2387.

- (3) Sakamoto, M.; Manseki, K.; Okawa, H. *Coord. Chem. Rev.* **2001**, *219–221*, 379–414.

- (4) Andruh, M.; Costes, J. P.; Diaz, C.; Gao, S. *Inorg. Chem.* **2009**, *48*, 3342–3359.

- (5) Costes, J. P.; Dahan, F.; Dupuis, A.; Laurent, J. P. *Inorg. Chem.* **2000**, *39*, 165–168.

- (6) (a) Colacio, E.; Ruiz, J.; Mota, A. J.; Palacios, M. A.; Cremades, E.; Ruiz, E.; White, F. J.; Brechin, E. K. *Inorg. Chem.* DOI: 10.1021/ic3004596; (b) Colacio, E.; Ruiz-Sanchez, J.; White, F. J.; Brechin, E. K. *Inorg. Chem.* **2011**, *50*, 7268–7273. (c) Yamaguchi, T.; Sunatsuki, Y.; Kojima, M.; Akashi, H.; Tsuchimoto, M.; Re, N.; Osa, S.; Matsumoto, N. *Chem. Commun.* **2004**, 1048–1049. (d) Yamaguchi, T.; Sunatsuki, Y.; Ishida, H.; Kojima, M.; Akashi, H.; Re, N.; Matsumoto, N.; Pochaba, A.; Mroziński, J. *Bull. Chem. Soc. Jpn.* **2008**, *81*, 598–605. (e) Yamaguchi, T.; Sunatsuki, Y.; Ishida, H.; Kojima, M.; Akashi, H.; Re, N.; Matsumoto, N.; Pochaba, A.; Mroziński, J. *Inorg. Chem.* **2008**, *47*, 5736–5745. (f) Costes, J. P.; Dahan, F.; Dupuis, A.; Laurent, J. P. *Inorg. Chem.* **1997**, *36*, 4284–4286. (g) Chandrasekhar, V.; Murugesu Pandian, B.; Boomishankar, R.; Steiner, A.; Vittal, J. J.; Houri, A.; Clérac, R. *Inorg. Chem.* **2008**, *47*, 4919–4929. (h) Barta, C. A.; Bayly, S. R.; Read, P. W.; Patrick, B. O.; Thompson, R. C.; Orvig, C. *Inorg. Chem.* **2008**, *47*, 2280–2293. (i) Shiga, T.; Ito, N.; Hidaka, A.; Okawa, H.; Kitagawa, S.; Ohba, M. *Inorg. Chem.* **2007**, *46*, 3492–3501. (j) Chen, Q. Y.; Luo, Q. H.; Zheng, L. M.; Wang, Z. L.; Chen, J. T. *Inorg. Chem.* **2002**, *41*, 605–609. (k) Pasatoiu, T. D.; Sutter, J. P.; Madalan, A. M.; Chiboub Fellah, F. Z.; Duhayon, C.; Andruh, M. *Inorg. Chem.* **2011**, *50*, 5890–5898. (l) Singh, S. K.; Tibrewal, N. K.; Rajaraman, G. *Dalton Trans.* **2011**, *40*, 10897–10906. (m) Costes, J. P.; Yamaguchi, T.; Kojima, M.; Vendier, L. *Inorg. Chem.* **2009**, *48*, 5555–5561. (n) Costes, J. P.; Vendier, L. *Eur. J. Inorg. Chem.* **2010**, 2768–2773. (o) Cimpoesu, F.; Dahan, F.; Ladeira, S.; Ferbinteanu, M.; Costes, J. P. *Inorg. Chem.* DOI: 10.1021/ic3001784.

- (7) Costes, J. P.; Dahan, F.; Dupuis, A.; Laurent, J. P. *Chem.—Eur. J.* **1998**, *4*, 1616–1620.

- (8) (a) Yamaguchi, T.; Costes, J. P.; Kishima, Y.; Kojima, M.; Sunatsuki, Y.; Bréfuel, N.; Tuchagues, J. P.; Vendier, L.; Wernsdorfer, W. *Inorg. Chem.* **2010**, *49*, 9125–9135. (b) Costes, J. P.; García-Tojal, J.; Tuchagues, J. P.; Vendier, L. *Eur. J. Inorg. Chem.* **2009**, 3801–3806.

- (9) Costes, J. P.; Clemente-Juan, J. M.; Dahan, F.; Dumestre, F.; Tuchagues, J. P. *Inorg. Chem.* **2002**, *41*, 2886–2891.

- (10) (a) Chandrasekhar, V.; Murugesu Pandian, B.; Azhakar, R.; Vittal, J. J.; Clérac, R. *Inorg. Chem.* **2007**, *46*, 5140–5142. (b) Huang, Y. G.; Wang, X. T.; Jiang, F. L.; Gao, S.; Wu, M. Y.; Gao, Q.; Wei, W.; Hong, M. C. *Chem.—Eur. J.* **2008**, *14*, 10340–10347. Chandrasekhar, V.; Murugesu Pandian, B.; Vittal, J. J.; Clérac, R. *Inorg. Chem.* **2009**, *48*, 1148–1157. Costes, J. P.; Vendier, L.; Wernsdorfer, W. *Dalton Trans.* **2011**, *40*, 1700–1706. Costes, J. P.; Dahan, F.; García-Tojal, J. *Chem.—Eur. J.* **2002**, *8*, 5430–5434.

- (11) (a) Costes, J.-P.; Auchel, M.; Dahan, F.; Peyrou, V.; Shova, S.; Wernsdorfer, W. *Inorg. Chem.* **2006**, *45*, 1924–1934. (b) Costes, J.-P.; Dahan, F.; Donnadiou, B.; Rodriguez-Douton, M. J.; Fernandez-Garcia, M. I.; Bousseksou, A.; Tuchagues, J. P. *Inorg. Chem.* **2004**, *43*, 2736–2744.

- (12) Gomez, V.; Vendier, L.; Corbella, M.; Costes, J. P. *Eur. J. Inorg. Chem.* **2011**, 2653–2656.

- (13) Richardson, M. F.; Wagner, W. F.; Sands, D. E. *J. Inorg. Nucl. Chem.* **1968**, *30*, 1275–1279.

- (14) Pascal, P. *Ann. Chim. Phys.* **1910**, *19*, 5–70.

- (15) Boudalis, A. K.; Clemente-Juan, J.-M.; Dahan, F.; Tuchagues, J.-P. *Inorg. Chem.* **2004**, *43*, 1574–1586.

- (16) (a) Borrás-Almenar, J. J.; Clemente-Juan, J. M.; Coronado, E.; Tsukerblat, B. S. *Inorg. Chem.* **1999**, *38*, 6081–6088. (b) Borrás-Almenar, J. J.; Clemente-Juan, J. M.; Coronado, E.; Tsukerblat, B. S. *J. Comput. Chem.* **2001**, *22*, 985–991.

- (17) James, F.; Roos, M. *Comput. Phys. Commun.* **1975**, *10*, 343–367.

- (18) *CrysAlis RED*, version 1.170.32; Oxford Diffraction Ltd.: Abingdon, U.K., 2003.

(19) SIR92 - A program for crystal structure solution; Altomare, A.; Casciarano, G.; Giacovazzo, C.; Guagliardi, A. *J. Appl. Crystallogr.* **1993**, *26*, 343–350.

(20) SHELX97 [Includes SHELXS97, SHELXL97, CIFTAB] - Programs for Crystal Structure Analysis (Release 97-2); Sheldrick, G. M. Institut für Anorganische Chemie, Universität Göttingen: Göttingen, Germany, 1998.

(21) WINGX - 1.63 Integrated System of Windows Programs for the Solution, Refinement and Analysis of Single Crystal X-Ray Diffraction Data; Farrugia, L. *J. Appl. Crystallogr.* **1999**, *32*, 837–840.

(22) *International tables for X-Ray crystallography*; Kynoch press: Birmingham, England, 1974; Vol IV.

(23) ORTEP3 for Windows; Farrugia, L. *J. Appl. Crystallogr.* **1997**, *30*, 565.

(24) Alvarez, S.; Llonell, M. *J. Chem. Soc., Dalton Trans.* **2000**, 3288–3303.

(25) Novitchi, G.; Wernsdorfer, W.; Chibotaru, L. F.; Costes, J. P.; Anson, A. E.; Powell, A. K. *Angew. Chem., Int. Ed.* **2009**, *48*, 1614–1619.

(26) (a) Costes, J. P.; Shova, S.; Wernsdorfer, W. *Dalton Trans.* **2008**, 1843–1849. (b) Costes, J. P.; Auchel, M.; Dahan, F.; Peyrou, V.; Shova, S.; Wernsdorfer, W. *Inorg. Chem.* **2006**, *45*, 1924–1934. (c) Kido, T.; Ikuta, Y.; Sunatsuki, Y.; Ogawa, Y.; Matsumoto, N.; Re, N. *Inorg. Chem.* **2003**, *42*, 398–408. (d) Kido, T.; Nagasato, S.; Sunatsuki, Y.; Matsumoto, N. *Chem. Commun.* **2000**, 2113–2114. (e) Costes, J. P.; Dahan, F. *C. R. Chim.* **2000**, *4*, 97–103.

(27) (a) Costes, J. P.; Dahan, F.; Dupuis, A. *Inorg. Chem.* **2000**, *39*, 5994–6000. (b) Costes, J. P.; Dahan, F.; Dupuis, A.; Laurent, J. P. *Inorg. Chem.* **2000**, *39*, 169–173. (c) Costes, J. P.; Vendier, L. *C. R. Chim.* **2010**, *13*, 661–667.

(28) Kobayashi, Y.; Ueki, S.; Ishida, T.; Nogami, T. *Chem. Phys. Lett.* **2003**, *378*, 337–342.

(29) Birk, T.; Pedersen, K. S.; Thuesen, C. A.; Weyhermüller, T.; Schau-Magnussen, M.; Piligkos, S.; Weihe, H.; Mossin, S.; Evangelisti, M.; Bendix, J. *Inorg. Chem.* **2012**, *51*, 5435–5443.

(30) Sanada, T.; Susuki, T.; Yoshida, T.; Kaizaki, S. *Inorg. Chem.* **1998**, *37*, 4712–4717.

(31) Rinck, J.; Novitchi, G.; Van der Heuvel, W.; Ungur, L.; Lan, Y.; Wernsdorfer, W.; Anson, C. E.; Chibotaru, L.; Powell, A. K. *Angew. Chem., Int. Ed.* **2010**, *49*, 7583–7587.

(32) (a) Shiga, T.; Onuki, T.; Matsumoto, T.; Nojiri, H.; Newton, G. N.; Hoshino, N.; Oshio, H. *Chem. Commun.* **2009**, 3568–3570. (b) Stamatatos, T. C.; Teat, S. J.; Wernsdorfer, W.; Christou, G. *Angew. Chem., Int. Ed.* **2009**, *48*, 521–524. (c) Bi, Y.; Li, Y.; Liao, W.; Zhang, H.; Li, D. *Inorg. Chem.* **2008**, *47*, 9733–9735. (d) Mereacre, V. M.; Ako, A. M.; Clérac, R.; Wernsdorfer, W.; Filoti, G.; Bartolomé, J.; Anson, C. E.; Powell, A. K. *J. Am. Chem. Soc.* **2007**, *129*, 9248–9249. (e) Mishra, A.; Wernsdorfer, W.; Parsons, S.; Christou, G.; Brechin, E. K. *Chem. Commun.* **2005**, 2086–2088. (f) Benelli, C.; Murrie, M.; Parsons, S.; Winpenny, E. P. *J. Chem. Soc., Dalton Trans.* **1999**, 4125–4126.

(33) Costes, J. P.; Dupuis, A.; Laurent, J. P. *Eur. J. Inorg. Chem.* **1998**, 1543–1546.

(34) Ferbinteanu, M.; Cimpoesu, F.; Girtu, M. A.; Enachescu, C.; Tanase, S. *Inorg. Chem.* **2012**, *51*, 40–50.

(35) Paulovic, J.; Cimpoesu, F.; Ferbinteanu, M.; Hirao, K. *J. Am. Chem. Soc.* **2004**, *126*, 3321–3331.